Konya Mühendislik Bilimleri Dergisi, c. 12, s.3, 725-736, 2024
Konya Journal of Engineering Sciences, v. 12, n. 3, 725-736, 2024
ISSN: 2667-8055 (Elektronic)
DOI: 10.36306/konjes.1517144

INVESTIGATION OF THE EFFECT OF ANNUAL AVERAGE TEMPERATURE AND PRECIPITATION CHANGES ON CORS-TR STATIONS: THE CASE OF KSTM STATION

[1]Alparslan ACAR, [2,*]Sercan BÜLBÜL, [3]Fuat BAŞÇİFTÇİ, [4]Ömer YILDIRIM

[1,4] Gaziosmanpasa University, Geomatics Engineering Department, Tokat, TÜRKİYE
[2] Konya Technical University, Geomatics Engineering Department, Konya, TÜRKİYE
[3]Karamanoglu Mehmetbey University, Mapping and Cadastre Programme, Karaman, TÜRKİYE
[1]alparslan.acar@gop.edu.tr, [2]sbulbul@ktun.edu.tr, [3]fuatbasciftci@kmu.edu.tr, [4]omer.yildirim@gop.edu.tr

Highlights

- Annual average temperature and precipitation changes
- CORS-TR stations covering the whole of Turkey are effectively used in earthquake researches to determine point positioning.
- GNSS is one of the most effective methods for determining point position by utilizing space technology.

***Corresponding Author:** Sercan BÜLBÜL, sbulbul@ktun.edu.tr

Konya Mühendislik Bilimleri Dergisi, c. 12, s.3, 725-736, 2024
Konya Journal of Engineering Sciences, v. 12, n. 3, 725-736, 2024
ISSN: 2667-8055 (Elektronic)
DOI: 10.36306/konjes.1517144

INVESTIGATION OF THE EFFECT OF ANNUAL AVERAGE TEMPERATURE AND PRECIPITATION CHANGES ON CORS-TR STATIONS: THE CASE OF KSTM STATION

[1]Alparslan ACAR, [2,*]Sercan BÜLBÜL, [3]Fuat BAŞÇİFTÇİ, [4]Ömer YILDIRIM

[1, 4] *Gaziosmanpasa University, Geomatics Engineering Department, Tokat, TÜRKİYE*
[2] *Konya Technical University, Geomatics Engineering Department, Konya, TÜRKİYE*
[3]*Karamanoglu Mehmetbey University, Mapping and Cadastre Programme, Karaman, TÜRKİYE*
[1]alparslan.acar@gop.edu.tr, [2]sbulbul@ktun.edu.tr, [3]fuatbasciftci@kmu.edu.tr, [4]omer.yildirim@gop.edu.tr

(Received: 17.07.2024; Accepted in Revised Form: 02.08.2024)

ABSTRACT: In this study, the effects of meteorological changes on the point positioning of CORS-TR stations were investigated. For this purpose, KURU, SINP, BOYT, CORU, CANK, CMLD, KRBK, KSTM stations were selected. The KSTM station was taken as unknown and adjusted based on other stations. Seasonal normal values of KSTM station in Kastamonu province covering the years 2016-2020 were examined in terms of temperature and precipitation amount. These values were determined according to the minimum, maximum and average value criteria by using Türkiye State Meteorological Service data. For the calculations, IGS-standardized RINEX data of the stations for 5 years and 12 months between 2016 and 2020 and for 10 days on the 11th and 20th days of each month were used. All calculations were processed with Leica Geo Office v8.x. The calculated coordinates were compared with the current coordinates of CORS-TR at the same epoch and examined according to annual temperature and precipitation. In the analyzes, it was tested by statistical method whether all measurements were compatible. When it was examined whether the temperature changes were statistically significant, it was observed that the test values were calculated according to the temperature changes were below the test distribution limit at 95% confidence interval. When it was examined whether the precipitation changes were statistically significant, it was observed that the test values were calculated according to the precipitation changes were below the test distribution limit at 95% confidence interval.

Keywords: *CORS-TR, GNSS, Leica Geo Office v8.x, Precipitation, Temperature*

1. INTRODUCTION

The Global Navigation Satellite System (GNSS), which is based on the principle of determining the location of a point on the Earth using instantaneous or different techniques, is becoming increasingly important in all areas of our lives. Here, while trying to obtain location information, many error sources that will affect the positioning accuracy may also occur. These; satellite clock and orbit errors, antenna phase center and receiver clock errors, atmospheric errors with ionospheric, tropospheric effects, errors due to signal reflection effect, etc. can be counted as. Elimination of these errors allows instantaneous and highly accurate position and velocity determination of a point on the earth.

GNSS technique applications in increasingly differentiated and diversified application areas such as navigation and transportation applications, meteorological studies, agriculture and hydrology fields, geodetic measurements, data collection for geographic information systems, remote sensing, geoscience studies have become a global monitoring system for collecting, evaluating and delivering data to many users for different methods in certain standards [1].

In addition to enabling both instant and post-process research on the subjects of study, these networks provide users with information such as ionosphere, troposphere corrections, time corrections, satellite orbital ephemeris, etc. The networks are improved, protected and maintained by different institutions/organizations. These networks include International GNSS Service (IGS), which is used globally, and the Continiously Operation Reference Stations-Türkiye (CORS-TR), which is used regionally in Türkiye and allows both post-process and continioulsy point positioning [2].

***Corresponding Author:** Sercan BÜLBÜL, sbulbul@ktun.edu.tr

In recent years, numerous studies have focused on the relationship between GNSS and meteorological changes under Space Weather Conditions (SWCs). The following citations are examples of some of such studies: Bilgen et al., [3], investigated the effect of Meteorological Weather Events on Precise Point Positioning at CORS-TR Stations. In the international paper prepared by Bos et al., [4], coordinates and velocities of 4 GNSS stations with continuous observations were found using time series. It is stated that the coordinates and velocities found have seasonal effects and what these effects are caused by.

Zumberge et al., [5] later proposed Precise Point Positioning (PPP) analysis in GNSS solutions. Nakamura et al., [6] mentioned that the Japanese GPS Earth Observation Network (GEONET) of more than 1200 GPS stations established for earthquake research has been expanded to include scientific applications, meteorology and ionospheric research, and GEONET contributes to the assimilation of GPS precipitable water vapor data into the Japan Meteorological Agency (JMA) Mesoscale Numerical Prediction Model. In the world, studies are ongoing to determine the appropriate model to be selected to obtain high-resolution water vapor distribution in small-scale areas for GNSS tomography [7-9].

Increasingly changing climatic conditions are discussed in national and international policies. In this context, studies are being carried out in various countries on the design and implementation of optimum systems for the prediction of meteorological disasters. This platform provides an overview into weather forecasting processes. This and similar studies will contribute to the identification of natural disasters related to meteorological events. National Center for Atmospheric Research and National Oceanic and Atmospheric Administration (NOAA) Forecast Systems Laboratory, Boulder, USA [10-12] and Department of Meteorology, Florida State University [13], Nottingham University and Met Office UK [14-15], Various meteorological institutions around the world, such as MeteoSwiss in Switzerland [16], the German Weather Service [17], the Danish Meteorological Institute, [18], the Finnish Meteorological Institute, [19], the French Meteorological Office [20], in Italy [21], and at the Shanghai Meteorological Center and the State Main Laboratory for Extreme Weather in collaboration with universities in China [22].

In this study, the effect of meteorological weather events on the location accuracy of the KSTM station between 2016 and 2020 was investigated. For this purpose, the coordinate change of the KSTM station for 5 years (11^{th} - 20^{th} days of each month) was analyzed by comparing space weather conditions and meteorological events.

2. MATERIAL AND METHOD

2.1. Space Weather Conditions and Indices

2.1.1. Space weather conditions

Unexpected irregular variations in the ionosphere of solar or extrasolar origin create space weather conditions. These include galactic cosmic rays, solar radiation storms, ionospheric scintillation, solar extreme ultraviolet (EUV) radiation, auroras, traveling ionospheric disturbance, coronal holes, geomagnetic storms, coronal mass ejection, radiation belts, solar flares and solar wind [23, 24]. These conditions are described in the subsections below and Figure 1 shows some of the space weather conditions and their effects [25].

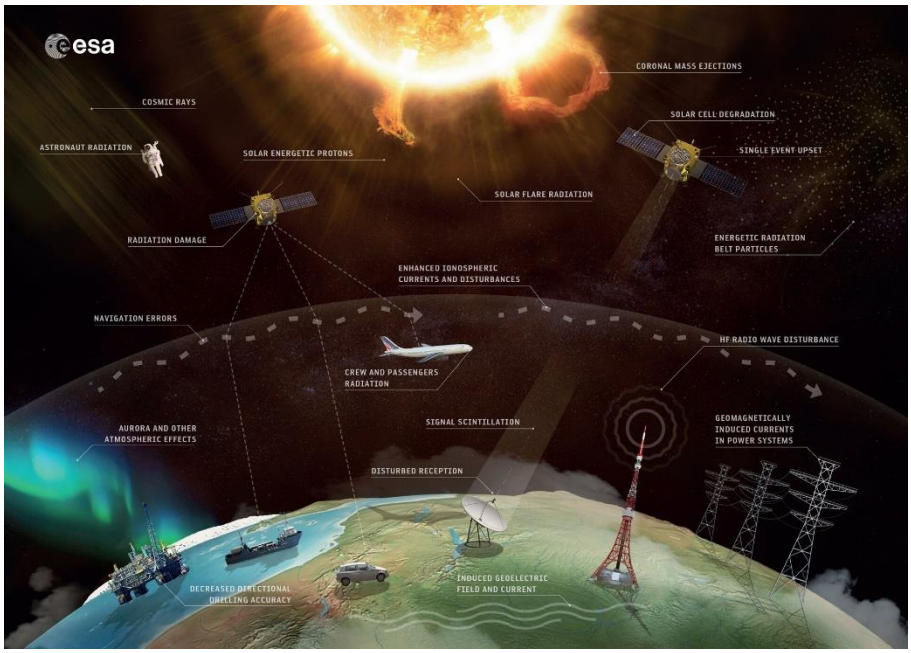

Figure 1. The effects of space weather conditions [25]

2.1.1.1. Solar activity indices

The most widely used index of solar activity, F10.7, has a wavelength of 10.7 cm (2800 MHz) and its unit is Solar Flux Units (sfu) [26]. As one of the most established records of solar activity, F10.7 has been measured since 1947 [27]. The F10.7 index is related to the Sunspot Number (SSN) [28]. F10.7 values vary over a wide range. It can be as low as 50 sfu during sunspot minimum periods and as high as 300 sfu during sunspot maximum periods. The threshold value of this index is 150 sfu, and if it exceeds this value, there is a situation of high solar activity (1 sfu=$10^{-22}$$Wm^{-2}Hz^{-1}$) [24].

2.1.1.2. Geomagnetic storm and geomagnetic activity indices

The geomagnetic storm (Kp) index, which stands for planetary index (planetarische Kennziffer), is used to measure and monitor changes in the Earth's magnetic field and to indicate the severity of disturbances in this field. It is also used to study the underlying causes of geomagnetic activity. The Kp index represents the average value of geomagnetic disturbance levels in two horizontal magnetic field components derived at 3-hour intervals, monitored by 13 ground-based magnetic observatories [29, 30]. The Kp index ranges from 0 to 9, where a value of 0 indicates minimal geomagnetic activity and a value of 9 indicates extreme geomagnetic storms [31].

One of the most common indices used to characterize geomagnetic activity is Disturbance storm time (Dst) and its unit is nanoTesla (nT). The index is a measure of the changes in the geomagnetic field during magnetic storms due to the influence of ring current originating in the terrestrial magnetosphere, which leads to a decrease in the horizontal component of the magnetic field. The Dst is obtained from the average of the distortions of the horizontal component (H component) of the Earth's magnetic field strength in the hourly range [32]. The Dst index, which determines whether a storm is occurring, is calculated from data from 4 observatories, Honolulu (21º19′1.2′′ North, 202° East), Kakioka (36º13′8′′ North, 140º11′20.4′′ East), San Juan (18º6′39.6′′ North, 293º51′00′′ East) and Hermanus (34º25′26.4′′ South, 19º13′30′′East) [33- 35].

2.2. Geolocations

There are two types of point positioning methods: absolute position and relative position determination.

Absolute position is the time elapsed between the signal time from the satellite and the arrival time at the receiver multiplied by the speed of light. Point positioning in this way is called absolute point positioning. The point positioning is calculated as follow;

$$\rho_a^u = \sqrt{(x_u - x_a)^2 + (y_u - y_a)^2 + (z_u - z_a)^2} = c.\Delta\delta_a^u \quad (1)$$

Here; x_u, y_u, z_u are satellite coordinates, x_a, y_a, z_a are the receiver coordinates and $\Delta\delta_u^a$ refers to the time difference between the receiver and the satellite.

The main purpose of the relative point positioning method is to eliminate common errors such as receiver clock errors, satellite clock errors and integer phase ambiguity. This is done by using a differencing approach between observations. The most commonly used differencing methods are single and double differencing (Figure 2).

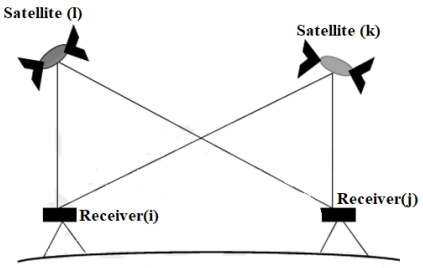

Figure 2. Observations between two receivers and two satellites

Single Differencing (SD) is a method that is performed by taking measurement differences between two receivers measuring to the same satellite or between two satellites and one receiver. This method eliminates clock errors. Single differences between two receivers and one satellite is obtained as;

$$\begin{aligned} \Delta L_{a_{ij}}^{u_l} &= L_{a_i}^{u_k} - L_{a_j}^{u_k} = \Delta\rho_{a_{ij}}^{u_k} + c\Delta\delta_{a_{ij}} + \Delta I_{a_{ij}}^{u_k} + \Delta\rho_{a_{ij}}^{u_k} + \Lambda\Delta N_{a_{ij}}^{u_k} + \varepsilon_{L_{ij}}^{k} \\ \Delta P_{a_{ij}}^{u_l} &= P_{a_i}^{u_k} - P_{a_j}^{u_k}\Delta\rho_{a_{ij}}^{u_k} + c\Delta\delta_{a_{ij}}\Delta I_{a_{ij}}^{u_k}\Delta\rho_{a_{ij}}^{u_k} + \varepsilon_{L_{ij}}^{k} \end{aligned} \quad (2)$$

This single differencing method between different receivers of the same satellite eliminates satellite clock errors. For short baselines up to a few kilometers, the ionospheric and tropospheric delay can be neglected due to the differential to the same satellite. A receiver is a single difference between two satellites is obtained as

$$\begin{aligned} \nabla L_{a_i}^{u_{kl}} &= L_{a_i}^{u_k} - L_{a_j}^{u_l} = \nabla\rho_{a_i}^{u_{kl}} + c\nabla\delta^{u_{kl}} + \nabla I_{a_i}^{u_{kl}} + \Delta\rho_{a_i}^{u_{kl}} + \Lambda\nabla N_{a_i}^{u_{kl}} + \varepsilon_{L_i}^{lk} \\ \nabla P_{a_i}^{u_{kl}} &= P_{a_i}^{u_k} - P_{a_j}^{u_l} = \nabla\rho_{a_i}^{u_{kl}} + c\nabla\delta^{u_{kl}} + \nabla I_{a_i}^{u_{kl}} + \Delta\rho_{a_i}^{u_{kl}} + \varepsilon_{P_i}^{lk} \end{aligned} \quad (3)$$

Receiver clock errors are eliminated by single differencing between different satellites and the same receiver [36].

3. DATASET

In this study, the effect of meteorological changes on the positions obtained from CORS-TR was investigated. The study area of the application was selected to cover a total of 8 CORS-TR, including KSTM

(Kastamonu) station in the center and other stations CMLD (Çamlıdere), KRBK (Karabük), KURU (Kurucaşile), SINP (Sinop), BOYT (Boyabat), CORU (Çorum), CANK (Çankırı) (Figure 3).

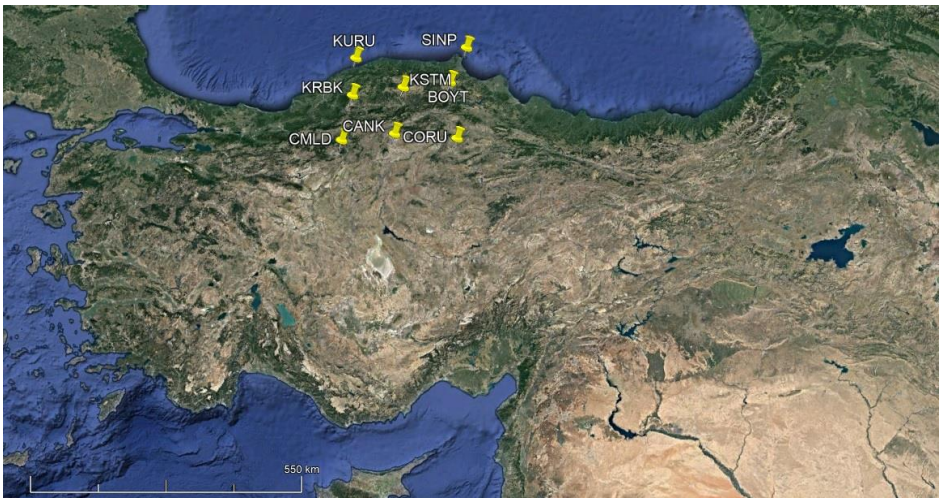

Figure 3. Application area and selected stations

While investigating the effect of meteorological changes on the positioning of CORS-TR in the study area, changes that may occur due to earthquake movements are not included in the analysis and evaluation.

The meteorological time intervals of the KSTM station (data are associated with Kastamonu province) in the study area were analyzed in two stages: temperature and precipitation. For this purpose, data on the monthly average temperature and monthly total precipitation amounts of the KSTM station point between 2016 and 2020 were obtained on the Meteorological data information presentation system (MEVBIS) of Türkiye State Meteorological Service (Figure 4-5).

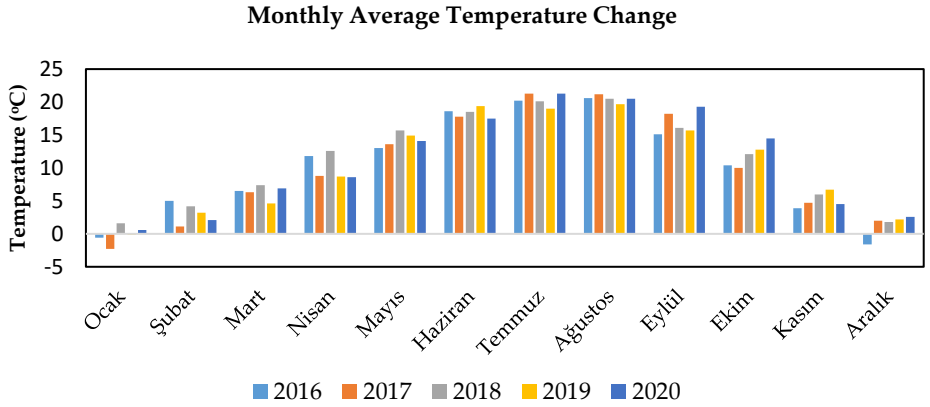

Figure 4. Monthly average temperature change between 2016 and 2020 for KSTM station

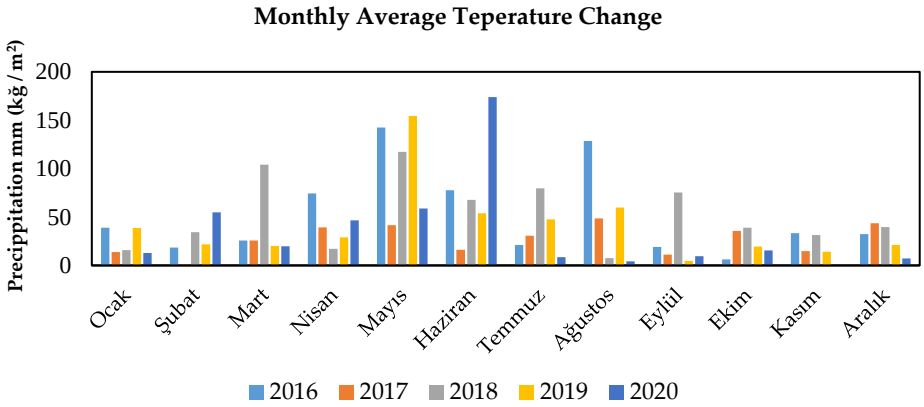

Figure 5. Monthly total precipitation change between 2016 and 2020 for KSTM station

When Figure 4-5 is analyzed, it is determined that January is the month with the lowest temperature and August is the month with the highest temperature between 2016 and 2020. In terms of monthly total precipitation amounts, it was observed that November was the month with the lowest precipitation and May was the month with the highest precipitation.

F10.7, Dst and Kp indices were obtained from https://omniweb.gsfc.nasa.gov/form/dx1.html.

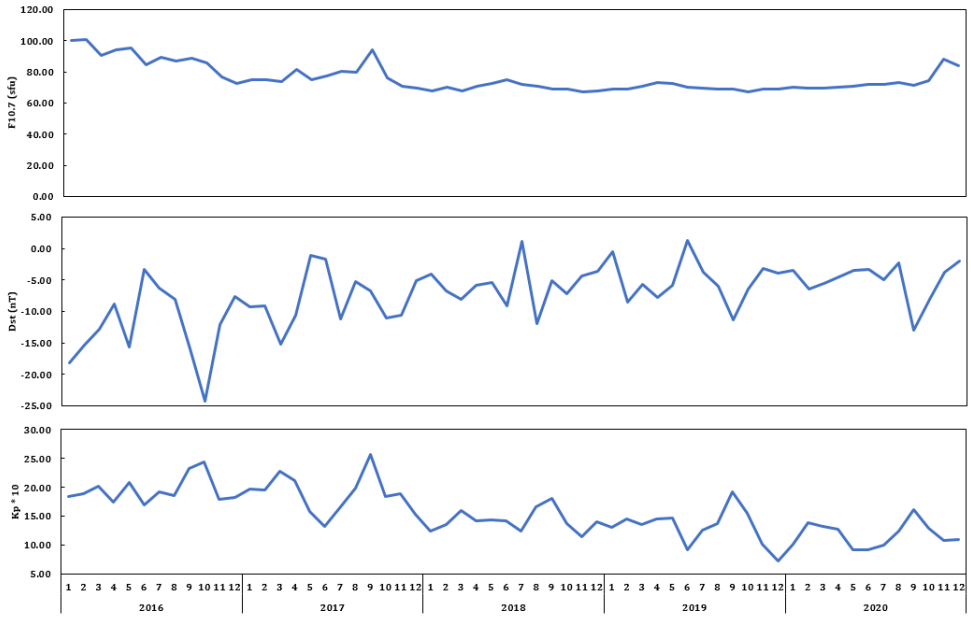

Figure 6. Space weather conditions between 2016 and 2020

When Figure 6 is analyzed, it is concluded that there is no disturbing activity on GNSS measurements in terms of space weather conditions in the selected date range and there is no other effect on coordinate calculations other than GNSS measurement errors.

In the analysis of position changes, 30-second, 24-hour RINEX data of CORS-TR and precise orbital information of GPS and GLONASS satellites (sp3) were used and daily solutions were obtained by processing GNSS data for the selected date range with Leica GeoOffice version 8.1 (LGO v8.1) software. Time series of daily solutions are given in Figure 7.

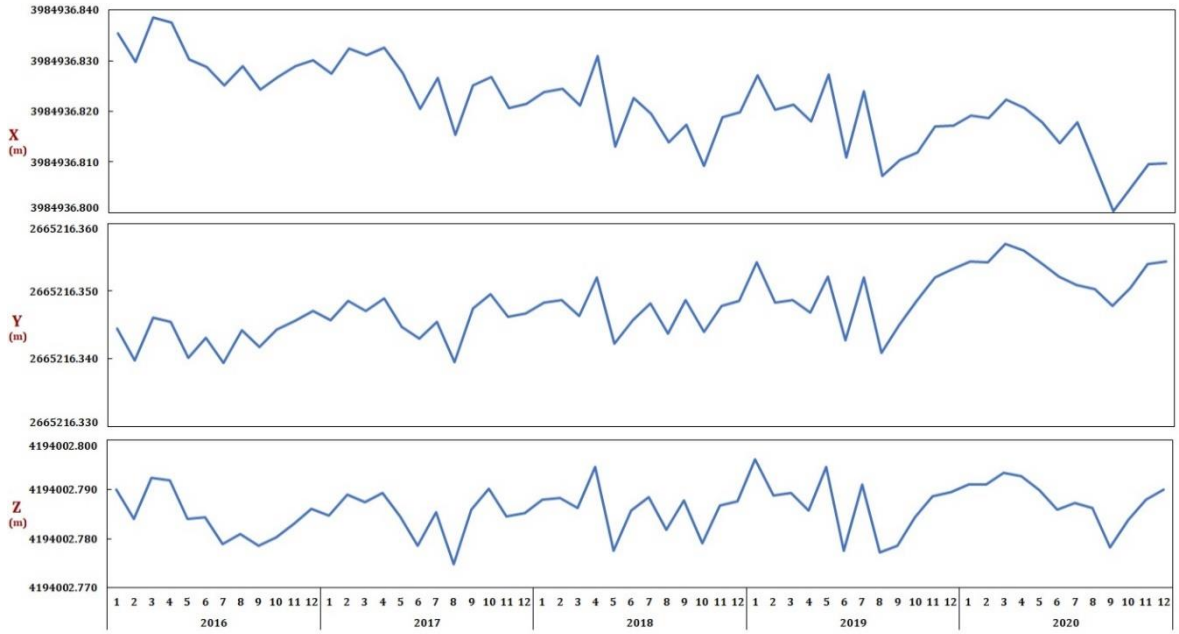

Figure 7. Coordinates of KSTM station between 2016 and 2020 (2005.0)

When Figure 7 is examined, it is seen that the X coordinate changed between 3984936.800 m - 3984936.839 m and there is a negative movement, the Y coordinate changed between 2665216.339 m - 2665216.357 m and there is a positive movement, and the Z coordinate changed between 4194002.775 m - 4194002.796 m.

4. RESULTS

The calculated coordinates of the KSTM station and the CORS-TR coordinates published by the General Directorate of Land Registry and Cadastre (TKGM) (2005.00 epoch) were compared and subjected to statistical testing at 95% confidence interval.

Using calculated coordinates and real coordinates (2005.00 epoch); differences of coordinates,

$$D_{X_{year}} = X_{i_{year}} - X_{2005.00} \quad D_{Y_{year}} = Y_{i_{year}} - Y_{2005.00} \quad D_{Z_{year}} = Z_{i_{year}} - Z_{2005.0} \tag{4}$$

root mean squared errors (RMSE) of the measures,

$$m_{X_{year}} = \sqrt{\frac{\left(\Sigma \mathrm{D}_{\mathrm{X_{year}}}\right)^2}{n}} \quad m_{Y_{year}} = \sqrt{\frac{\left(\Sigma \mathrm{D}_{\mathrm{Y_{year}}}\right)^2}{n}} \quad m_{Z_{year}} = \sqrt{\frac{\left(\Sigma \mathrm{D}_{\mathrm{Z_{year}}}\right)^2}{n}} \tag{5}$$

RMSEs of the differences

$$\begin{aligned} m_{DX} &= \sqrt{\left(m_{X_{2016}}\right)^2 + \left(m_{X_{2017}}\right)^2 + \left(m_{X_{2018}}\right)^2 + \left(m_{X_{2019}}\right)^2 + \left(m_{X_{2020}}\right)^2} \\ m_{DY} &= \sqrt{\left(m_{Y_{2016}}\right)^2 + \left(m_{Y_{2017}}\right)^2 + \left(m_{Y_{2018}}\right)^2 + \left(m_{Y_{2019}}\right)^2 + \left(m_{Y_{2020}}\right)^2} \\ m_{DZ} &= \sqrt{\left(m_{Z_{2016}}\right)^2 + \left(m_{Z_{2017}}\right)^2 + \left(m_{Z_{2018}}\right)^2 + \left(m_{Z_{2019}}\right)^2 + \left(m_{Z_{2020}}\right)^2} \end{aligned} \tag{6}$$

and test values;

$$T_X = \frac{D_X}{m_{DX}} \qquad T_Y = \frac{D_Y}{m_{DY}} \qquad T_Z = \frac{D_Z}{m_{DZ}} \tag{7}$$

calculated with the equations.

Figure 8 shows the calculated Cartesian coordinate differences of the KSTM station, and Tables 2-4 show the test values and RMSE of the measurements and differences.

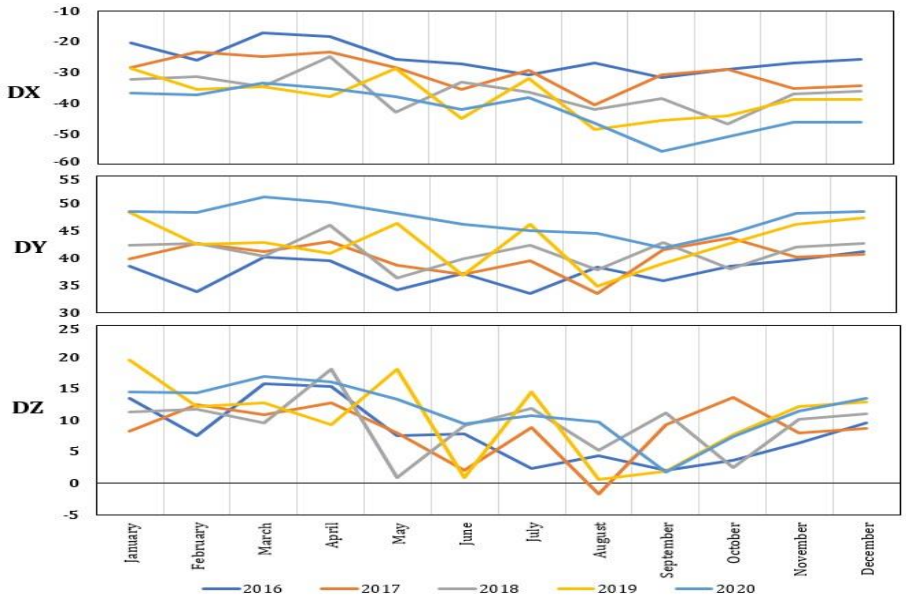

Figure 8. Cartesian coordinate differences (mm) for KSTM station

Table 1. KSTM station between 2016 and 2020 D_X statistical values of the coordinate difference

	2016		2017		2018		2019		2020	
	D_X (mm)	T_X	D_X (mm)	T_X	D_X (mm)	T_X	D_X (mm)	T_X	D_X (mm)	T_X
January	-20.64	0.26	-28.54	0.36	-32.24	0.41	-28.84	0.36	-36.84	0.46
February	-26.17	0.33	-23.57	0.30	-31.57	0.40	-35.67	0.45	-37.37	0.47
March	-17.40	0.22	-24.95	0.31	-34.85	0.44	-34.75	0.44	-33.70	0.42
April	-18.53	0.23	-23.48	0.30	-25.08	0.32	-37.98	0.48	-35.33	0.44
May	-25.81	0.32	-28.45	0.36	-42.98	0.54	-28.75	0.36	-38.11	0.48
June	-27.24	0.34	-35.58	0.45	-33.28	0.42	-45.18	0.57	-42.24	0.53
July	-30.92	0.39	-29.46	0.37	-36.56	0.46	-31.96	0.40	-38.22	0.48
August	-27.05	0.34	-40.69	0.51	-42.19	0.53	-48.79	0.61	-46.65	0.59
September	-31.78	0.40	-30.92	0.39	-38.72	0.49	-45.62	0.57	-55.68	0.70
October	-29.25	0.37	-29.20	0.37	-46.80	0.59	-44.10	0.55	-51.05	0.64
November	-27.09	0.34	-35.33	0.44	-37.13	0.47	-39.03	0.49	-46.39	0.58
December	-25.96	0.33	-34.51	0.43	-36.21	0.46	-38.81	0.49	-46.26	0.58
$m_{d_{x_i}}$	26.02		30.81		36.89		38.81		42.83	
m_{D_X}					79.55					

Table 2. KSTM station between 2016 and 2020 D_Y statistical values of the coordinate difference

	2016		2017		2018		2019		2020	
	D_Y (mm)	T_Y	D_Y (mm)	T_Y	D_Y (mm)	T_Y	D_Y (mm)	T_Y	D_Y (mm)	T_Y
January	38.61	0.49	39.81	0.50	42.41	0.53	48.31	0.61	48.51	0.61
February	33.87	0.43	42.67	0.54	42.77	0.54	42.47	0.53	48.37	0.61
March	40.19	0.51	41.22	0.52	40.42	0.51	42.82	0.54	51.09	0.64
April	39.55	0.50	42.98	0.54	46.08	0.58	40.88	0.51	50.15	0.63
May	34.24	0.43	38.76	0.49	36.36	0.46	46.26	0.58	48.24	0.61
June	37.19	0.47	37.12	0.47	39.82	0.50	36.82	0.46	46.19	0.58
July	33.48	0.42	39.51	0.50	42.31	0.53	46.11	0.58	44.98	0.57
August	38.34	0.48	33.56	0.42	37.86	0.48	34.96	0.44	44.44	0.56
September	35.80	0.45	41.52	0.52	42.82	0.54	39.02	0.49	41.90	0.53
October	38.48	0.48	43.61	0.55	38.11	0.48	42.71	0.54	44.58	0.56
November	39.64	0.50	40.27	0.51	41.97	0.53	46.17	0.58	48.14	0.61
December	41.22	0.52	40.76	0.51	42.66	0.54	47.36	0.60	48.52	0.61
$m_{d_{y_i}}$	37.63		40.24		41.21		43.02		47.16	
m_{D_Y}					93.85					

Table 3. KSTM station between 2016 and 2020 D_Z statistical values of the coordinate difference

	2016		2017		2018		2019		2020	
	D_Z (mm)	T_Z	D_Z (mm)	T_Z	D_Z (mm)	T_Z	D_Z (mm)	T_Z	D_Z (mm)	T_Z
January	13.38	0.17	8.18	0.10	11.28	0.14	19.48	0.24	14.38	0.18
February	7.46	0.09	12.46	0.16	11.76	0.15	12.16	0.15	14.36	0.18
March	15.78	0.20	10.80	0.14	9.60	0.12	12.70	0.16	16.88	0.21
April	15.26	0.19	12.68	0.16	18.08	0.23	9.18	0.12	16.06	0.20
May	7.46	0.09	7.88	0.10	0.88	0.01	18.08	0.23	13.26	0.17
June	7.74	0.10	1.96	0.02	9.06	0.11	0.86	0.01	9.34	0.12
July	2.34	0.03	8.86	0.11	11.86	0.15	14.46	0.18	10.74	0.14
August	4.32	0.05	-1.76	0.02	5.14	0.06	0.64	0.01	9.72	0.12
September	2.00	0.03	9.32	0.12	11.12	0.14	1.92	0.02	1.70	0.02
October	3.60	0.05	13.62	0.17	2.42	0.03	7.72	0.10	7.30	0.09
November	6.38	0.08	8.00	0.10	10.10	0.13	12.10	0.15	11.38	0.14
December	9.48	0.12	8.70	0.11	11.00	0.14	12.90	0.16	13.38	0.17
$m_{d_{z_i}}$	9.15		9.39		10.36		11.85		12.23	
m_{D_Z}					23.86					

The test distribution limit of the calculated test magnitudes at 95% confidence interval $t_{f,1-0.05/2} = 2.5706$ with the limit value. When Table 1-3 is examined, it is seen that all test values are compared with the limit value $t_{f,1-0.05/2}$ and it was observed that it remained smaller than table value.

5. CONCLUSION

The meteorological time intervals of the KSTM station located in the study area were evaluated in two stages: temperature and precipitation. For this purpose, data on the monthly average temperature and monthly total precipitation amounts of Kastamonu province between 2016-2020, where KSTM station is located, were obtained from the MEVBIS. As a result of the study, when the average temperature is examined periods between 2016-2020, it was concluded that the month with the lowest temperature was January with -0.16 °C, the month with the highest temperature was August with 20.5 °C, and when the monthly total precipitation amounts were examined; the month with the lowest amount of precipitation was November with 18.94 (mm) and the month with the highest amount of precipitation was May with 102.90 (mm).

When Figure 6 is analyzed again, it is concluded that there is no disturbing activity on GNSS measurements in terms of space weather conditions in the selected date range and there is no other effect on coordinate calculations other than GNSS measurement errors. The data were processed in LGO v8.1

software by using 30-s and 24-hour RINEX data of CORS-TR for ten days starting from the 11th day of the month for the months of January, May, August and November and the precise orbit ephemeris information of GPS and GLONASS satellites. In the next stage, velocity vector were calculated and the coordinates of the KSTM station were shifted to the reference epoch (ITRF96 2005.00 Epoch). These coordinates were compared with the real coordinates published by the TKGM and subjected to statistical test at 95% confidence interval.

When it was examined whether the temperature changes were statistically significant, it was observed that the test values were calculated according to the temperature changes were below the test distribution limit $t_{f,1-0.05/2} = 2.5706$ at 95% confidence interval. As a result, it is seen that the positioing changes of the KSTM station within the study boundary are not affected by the temperature changes during the selected years.

When it was examined whether the precipitation changes were statistically significant, it was observed that the test values were calculated according to the precipitation changes were below the test distribution limit $t_{f,1-0.05/2} = 2.5706$ at 95% confidence interval. As a result, it is seen that the positioning changes of the KSTM station within the study boundary are not also affected by the precipitation during the years.

As a result of this study, it was observed that temperature and precipitation changes did not have any negative effect on positioning with CORS-TR stations. As a result, it was found that the measurements made based on the CORS-TR network in all weather conditions give equal accuracy. In this study, the fact that the selected days did not exceed the limit values in any space weather conditions could not reveal the relationship between GNSS and positioning. In order to guide future studies, it would be appropriate to investigate the possible effects of different space weather conditions on GNSS position accuracy.

Declaration of Ethical Standards

The authors declare that the study complies with all applicable laws and regulations and meets ethical standards.

Declaration of Competing Interest

The authors declare that they have no known competing financial interests or personal relationships that could have appeared to influence the work reported in this paper.

Funding / Acknowledgements

The authors declare that no funding was used in the study.

Data Availability

No data are associated in the manuscript.

6. REFERENCES

[1] F. Pektaş, "Gerçek zamanlı ulusal ve yerel Sabit GNSS ağlarına dayalı kinematik konumlama (TUSAGA-Aktif – İSKİ-UKBS ağlarının yerel ölçekte karşılaştırılması," M. S. thesis, Yildiz Technical University, Istanbul, 2010.

[2] S. Bülbül, "TUSAGA-Aktif noktalarında renkli gürültülerden arındırılmış hız bileşenlerinin belirlenmesi," Ph. D. thesis, Konya Technical University, Konya, 2018.

[3] B. Bilgen, S. Bülbül, and C. İnal C. "TUSAGA-Aktif istasyonlarındaki meteorolojik hava olaylarının hassas nokta konumlamaya etkisi," *Afyon Kocatepe Üniversitesi Fen ve Mühendislik Bilimleri Dergisi*, vol. 21, no. 6, pp. 1393-1403, 2021.

[4] M. S. Bos, L. Bastos, and R.M.S. Fernandes, "The ınfluence of seasonal signals on the estimation of the tectonic motion in short continuous GPS time-series," *Journal of Geodynamics*, vol. 49, pp. 205-209, 2010.

[5] J.F. Zumberge, M.B. Heflin, D. C. Jefferson, M.M. Watkins, and F.H. Webb, "Precise point processing for the efficient and robust analysis of GPS data from large networks," *Journal of Geophysical Research*, vol. 102, pp. 5005-5017, 1997.

[6] H. Nakamura, K. Koizumi, and N. Mannoji, "Data Assimilation of GPS precipitable water vapor into the jma mesoscale numerical weather prediction model and ıts ımpact on rainfall forecasts," *Journal of the Meteorological Society of Japan*, vol. 82, no. 1, pp. 441–452, 2004.

[7] G. Möller, and D. Landskron, "Atmospheric bending effects in GNSS tomography," *Atmospheric Measurement Techniques*, vol. 12, no. 1, pp, 23–34, 2019.

[8] A. Garcia Vieira de Sá, "Tomographic determination of the spatial distribution of water vapour using GNSS observations for real-time applications," Ph. D. thesis, Wrocław University of Environmental and Life Sciences, 2018.

[9] H. Brenot, W. Rohm, M. Kačmařík, G. Möller, A. Sá, D. Tondaś, L. Rapant, R. Biondi, T. Manning, and C. Champollion, "Cross-comparison ve methodological ımprovement in GPS tomography," *Remote Sensing*, vol. 12, no. 1, pp. 30, 2020.

[10] Y. H. Kuo, Y.R. Guo, and E.R. Westwater, "Assimilation of precipitable water measurements into a mesoscale numerical model," *Monthly Weather Review*, vol. 121, no. 4, pp. 1215-1238, 1993.

[11] T. L. Smith, S. G. Benjamin, S. I. Gutman, and S. Sahm, "Short-range forecast ımpact from assimilation of GPS-IPW observations into the rapid update cycle," *Monthly Weather Review*, vol. 135, no.8, pp. 2914-2930, 2007.

[12] M.S. F. V. De Pondeca, and X. Zou, "A case study of the variational assimilation of GPS zenit delay observations into a mesoscale model," *Journal of Applied Meteorology and Climatology*, vol. 40, no. 9, pp. 1559-1576, 2001.

[13] S. Q. Peng, and X. Zou, "Impact on short-range precipitation forecasts from assimilation of ground-based GPS zenit total delay and rain gauge precipitation observations," *Journal of the Meteorological Society of Japan*, vol. 82, no. 1B, pp. 491-506, 2004.

[14] H.C. Baker, A. H. Dodson, N.T. Penna, M. Higgings, and D. Offiler, "Ground-based GPS water vapour estimation: potential for meteorological forecasting," *Journal of Atmospheric and Solar-Terrestrial Physics*, vol. 63, no. 12, pp. 1305-1314, 2001.

[15] D. Jerrett, and J. Nash, "Potential uses of surface based GPS water vapour measurements for meteorological purposes," *Physics and Chemistry of the Earth, Part A: Solid Earth and Geodesy*, vol. 6, no. 6-8, pp. 457- 461, 2001.

[16] G. Guerova, "Application of GPS derived water vapour for numerical weather prediction in switzerlve," Ph. D. thesis, University of Bern, 2003.

[17] G. Gendt, G. Dick, C. Reigber, M. Tomassini, Y. Liu, and M. Ramatschi, "Near real time GPS water vapor monitoring for numerical weather prediction in Germany," *Journal of the Meteorological Society of Japan*, vol. 82, no. 1B, pp. 361-370, 2004.

[18] H. Vedel, and X. Y. Huang, "Impact of ground based GPS data on numerical weather prediction," *Journal of the Meteorological Society of Japan*, vol. 82, no. 1B, pp. 459–472, 2004.

[19] R. Eresmaa, H. Järvinen, and K. Salonen, "Potential of ground-based GPS slant delays for numerical weather prediction," *Atmos. Chem. Phys.*, vol. 7, pp. 3143–3151, 2006.

[20] P. Poli, P. Moll, F. Rabier, G. Desroziers, B. Chapnik, L. Berre, S. B. Healy, E. Andersson, and F. Z. ElGuelai, "Forecast impact studies of zenit total delay data from european near real-time GPS stations in météo France 4DVAR," *Journal of Geophysical Research: Atmospheres*, vol. 112, pp. D06114, 2007.

[21] C. Faccani, R. Ferretti, R. Pacione, T. Paolucci, F. Vespe, and L. Cucurull, "Impact of a high density GPS network on the operational forecast," *Advances in Geosciences*, vol. 2, pp. 73-79, 2005.

[22] M. Zhang, Y. Ni, and F. Zhang, "Variational assimilation of GPS precipitable water vapor ve hourly rainfall observations for a Meso-β scale heavy precipitation event during the 2002 Mei-Yu Season," *Advances in Atmospheric Sciences*, vol. 24, no. 3, pp. 509-526, 2007.

[23] National Oceanic and Atmospheric Administration, "Space Weather Predıctıon Center," [Online]. Available: https://www.swpc.noaa.gov/phenomena [Accessed: Apr. 20, 2024].

[24] F. Başçiftçi, C. Inal, Ö. Yildirim, and S. Bulbul, "Comparison of regional and global TEC values: Turkey model," *International Journal of Engineering and Geosciences*, vol. 3, no. 2, pp. 61-72, 2018.

[25] ESA Space Weather Service Network, [Online]. Available: https://swe.ssa.esa.int/what-is-space-weather [Accessed: May. 15, 2024].

[26] R. Mukesh, V. Karthikeyan, P. Soma, and P. Sindhu, "Cokriging based statistical approximation model for forecasting ionospheric VTEC during high solar activity and storm days," *Astrophysics and Space Science*, vol. 364, pp. 131, 2019.

[27] Space Weather Predıctıon Center (2024). F10.7 cm radio emissions, [Online]. Available: https://www.swpc.noaa.gov/phenomena/f107-cm-radio-emissions [Accessed: May. 16, 2024].

[28] Australian Space Weather Forecasting Centre [Online]. Available: https://www.sws.bom.gov.au/ [Accessed: May. 16, 2024].

[29] International Service of Geomagnetic Indices, "Kp index," [Online]. Available: https://isgi.unistra.fr/indices_kp.php [Accessed: May. 16, 2024].

[30] F. Basciftci, and S. Bulbul, "Investigation of ionospheric TEC changes potentially related to Seferihisar-Izmir earthquake (30 October 2020, MW 6.6)," *Bulletin of Geophysics & Oceanography*, vol. 63, no. 3, pp. 4382–4400, 2022.

[31] B. Lemmerer, S. Unger, "Modeling and pricing of space weather derivatives," *Risk Management*, vol. 21, pp. 265–291, 2019.

[32] N. Myagkova, V. R. Shirokii, R. D. Vladimirov, O. G. Barinov, and S. A. Dolenko, "Prediction of the Dst geomagnetic index using adaptive methods," *Russian Meteorology and Hydrology*, vol. 46, pp. 157–162, 2021.

[33] International Service of Geomagnetic Indices "Dst index", [Online]. Available: https://isgi.unistra.fr/indices_dst.php [Accessed: May. 16, 2024].

[34] Banerjee, A. Bej, and T. N. Chatterjee, "On the existence of a long range correlation in the Geomagnetic Disturbance storm time (Dst) index," *Astrophysics and Space Science*, vol. 337, pp. 23–32, 2012.

[35] S. Bulbul, and F. Basciftci, "TEC anomalies observed before and after Sivrice-Elaziğ earthquake (24 January 2020, Mw: 6.8)," *Arabian Journal of Geosciences*, vol. 14, no. 12, pp. 1077, 2021.

[36] R. Dach, S. Lutz, P. Walser, and P. Fridez, *Bernese GNSS Software Version 5.2. User manual*, Astronomical Institute, University of Bern, Bern Open Publishing, 2015.